NJC

Accepted Manuscript

This article can be cited before page numbers have been issued, to do this please use: L. N. Neupane, P. K. Mehta and K. Lee, *New J. Chem.*, 2017, DOI: 10.1039/C6NJ03830A.

This is an Accepted Manuscript, which has been through the Royal Society of Chemistry peer review process and has been accepted for publication.

Accepted Manuscripts are published online shortly after acceptance, before technical editing, formatting and proof reading. Using this free service, authors can make their results available to the community, in citable form, before we publish the edited article. We will replace this Accepted Manuscript with the edited and formatted Advance Article as soon as it is available.

You can find more information about Accepted Manuscripts in the author guidelines.

Please note that technical editing may introduce minor changes to the text and/or graphics, which may alter content. The journal's standard Terms & Conditions and the ethical guidelines, outlined in our author and reviewer resource centre, still apply. In no event shall the Royal Society of Chemistry be held responsible for any errors or omissions in this Accepted Manuscript or any consequences arising from the use of any information it contains.

ROYAL SOCIETY OF CHEMISTRY

rsc.li/njc

View Article Online
DOI: 10.1039/C6NJ03830A

NJC

Sensitive and selective ratiometric fluorescent detection of monosaccharides in aqueous solutions at physiological pH using self-assembled peptides with different aromatic side chains

Received 00th January 20xx,
Accepted 00th January 20xx

DOI: 10.1039/x0xx00000x

www.rsc.org/

Lok Nath Neupane, Pramod Kumar Mehta, and Keun-Hyeung Lee*

The control of disassembly of supramolecular nanostructures of the self-assembled peptides by specific stimuli has not been intensively investigated for the fluorescent detection of the analytes in aqueous solutions. In the present study, we investigated the control of assembly and disassembly of self-assembled peptides by monosaccharides for the ratiometric detection. A series of amphiphilic dipeptides (**1**–**4**) with a different aromatic side chain bearing a phenylboronic acid and pyrene fluorphore were synthesized. The dipeptides (**1**–**3**) spontaneously self-aggregated and formed nanoparticles in aqueous solutions, resulting in the significant pyrene excimer emissions, whereas the dipeptide (**4**) did not aggregate, resulting in a little excimer emission. The addition of sugars induced the disassembly of the self-aggregates of **1**–**3**, resulting in a decrease in excimer emission and an increase in monomer emission. All peptides (**1**-**4**) showed a high selectivity for fructose among monosaccharides and **3** showed the lowest detection limit for fructose among the peptides showed ratiometric responses. The addition of a hydrophobic pinanediol stabilized the self-aggregates of **1**–**3**, resulting in an increase in excimer emission and a decrease in monomer emission. Even though **4** did not self-aggregate in aqueous solution, the addition of pinanediol induced the assembly of nanoparticles, resulting in a significant increase of excimer emission and a decrease of monomer emissions. The results revealed that the assembly and disassembly of the self-assembled peptides could be controlled by covalent bonding with sugar, which was suitable for the sensitive ratiometric detection of monosaccharides in aqueous solutions at physiological pH.

Introduction

Supramolecular structures of the self-assembly of small biomolecules played a critical role for the specific biological functions in living systems. The self-assembled peptides that can form supramolecular structures have been extensively studied for the potential use in diverse applications such as drug delivery, tissue engineering, bioelectronics, and sensing due to easy synthesis, high biocompatibility, and various functionalities of peptides.[1–4] As the self-assembled peptides could form a various well-defined nanostructures such as nanoparticles, nanofiber, nanorods, and nanotubes, control of the primary structures of the self-assembled peptides for the specific nanostructures have been extensively investigated.[1–11]

In recent years, triggers for the assembly of the self-assembled peptides by external stimuli have been the focus of much research. The self-assembled peptides have been further designed with triggers for the assembly of various nanostructures by various stimuli such as solvent, pH, temperature, salt concentration, metal ions, and enzymes.[12–20] Even though assembly as well as disassembly processes was important for the various applications including drug delivery and detection of analytes, the disassembly of supramolecular nanostructures of the self-assembled peptide by specific stimuli has not been intensively investigated for the sensing systems. Monosaccharides are essential biomolecules because they played significant roles in various biological processes such as signal transduction, cell–cell interactions, bacteria–host interactions, fertility, and development.[21,22] Thus, the control of disassembly and assembly of the self-assembled peptides by monosaccharides should be important for further applications including sensing. However, it is rarely reported that the self-assembled peptides was used a new sensing system for monosaccharides in aqueous solutions.

Fluorescence has received great attention for the detection of analytes due to inexpensive instrument, simple, rapid, and high sensitivity. A variety of fluorescent probes for monosaccharides has been reported.[23–36] However, most of the probes showed turn-on responses to sugars, whereas a few of the probes showed ratiometric responses to sugars and most of the ratiometric probes required a tedious synthesis.[23–36] Turn-on response was more preferred than turn-off response because turn-off response could not be differentiated with the false signals induced by the precipitation of the sensors or the absorbance of impurities. However, turn on responses using one emission band were affected by environmental effects such as pH, polarity of the media, and temperature.[37,38] Ratiometric responses using two different emission bands were highly recommended because the ratio between two emission intensities could correct the environmental effects. However, most of ratiometric probes for monosaccharides required a difficult synthesis and did not show sensitive responses to sugar in aqueous solutions at physiological pH. Furthermore, considering the real applications of the fluorescent probe, a relatively large emission change by target analytes was highly

Bioorganic chemistry Lab, Center for Design and Applications of Molecular Catalysts, Department of Chemistry and Chemical Engineering, Inha University, 100 Inha-Ro, Yonghyun Dong, Nam-Gu, Incheon 402-751, Republic of Korea
E-mail: leekh@inha.ac.kr
† Electronic Supplementary Information (ESI) available: Characterization and additional data of compounds are provided. See DOI: 10.1039/x0xx00000x

View Article Online
DOI: 10.1039/C6NJ03830A
Paper NJC

recommended. However, the recent reported ratiometric probe showed a relatively small emission change and/or intensity ratio change by monosaccharides at physiological pH. Thus, it is highly challenging for the design of fluorescent probes with easy synthesis that show sensitive ratiometric responses to monosaccharides with significant emission intensity changes in aqueous solutions at physiological pH.

Since Gazit et al. reported that the self-assembled dipeptide consisting of PhePhe aggregated and formed a range of different nanostructures including nanoparticles, nanofibril, nanorods, nanotubular aggregates in different solvent conditions,[2,39] short self-assembled peptides have received attentions as biomaterials for drug delivery systems, bioelectronics, and tissue engineering.[1–4] However, the control of the assembly and disassembly of the self-assembled peptides by carbohydrates was rarely investigated.[40–42] In the previous research, we proposed a new ratiometric sensing system for monosaccharides based on the fluorescent dipeptide bearing a phenylboronic acid.[43] Furthermore, unlike the chemical probes, the sensitivity, the response type, and selectivity of the peptide-based probes for specific targets can be easily optimized by further tuning of the amino acid sequences of the peptide part.

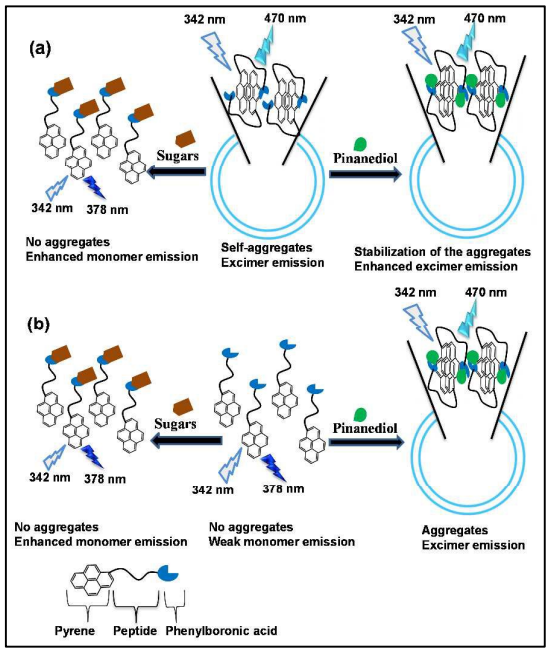

Scheme 1. Proposed binding mode of (a) **1**–**3** and (b) **4** with sugars and pinanediol for fluorescent change and aggregations.

In the present study, we synthesized several self-assembled dipeptides bearing a phenylboronic acid as a receptor and investigated the control of assembly and disassembly of the self-assembled peptides by monosaccharides and a hydrophobic diol compound for the ratiometric sensing (Scheme 1). Dipeptides (**1**–**3**) bearing a phenylboronic acid self-aggregated and formed nanoparticles in aqueous solutions at physiological pH. Upon addition of hydrophilic monosaccharides, the nanoparticles of the dipeptides (**1**–**3**) were disassembled, resulting in the increase of monomer emissions at 378 nm and concomitant decrease of the excimer emissions at 470 nm. Among the peptide-based probes (**1**–**3**) showed ratiometric responses to monosaccharides, **3** showed the lowest detection limit for fructose and exhibited a selective ratiometric response to fructose among the tested monosaccharides. The dipeptide (**4**) that did not aggregate in aqueous solutions at physiological pH, showed a turn on response to monosaccharide however exhibited a ratiometric response to pinanediol by the increase of excimer emissions and decrease of monomer emissions. The present study provides a new sensing system based on the self-assembled peptides for the sensitive ratiometric detections for monosaccharides in aqueous solutions at physiological pH.

Experimental

Materials

Fmoc-Orn(alloc)-OH and Fmoc-NaI-OH were purchased from Bachem. Fmoc-Trp(Boc)-OH, Fmoc-Phe-OH, Fmoc-His(Trt)-OH, Rink Amide MBHA resin, 1-hydroxybenzotriazole (HOBt) and N,N''-diisopropylcarbodiimide (DIC) were purchased from Bead Tech. 1-pyreneacetic acid, 4-Carboxyphenylboronic acid pinacol ester, trifluoroacetic acid (TFA), N,N'-dimethylformamide (DMF), Dichloromethane (DCM), Tetrakis(triphenylphosphine) palladium(0) Pd(PPh3)4, Phenylsilane, (1S,2S,3R,5S)-(+)-pinanediol, piperidine were purchased from Sigma Aldrich.

Solid phase synthesis of compounds

The peptides were synthesized by solid phase synthesis with Fmoc chemistry.[44] Fmoc protected L-Trp(Boc)-OH, Fmoc-NaI-OH, Fmoc-Phe- OH and Fmoc-His (Trt)-OH (0.3 mmol of each, 3 equiv) were separately assembled on Rink Amide MBHA resin (0.1 mmol) for the synthesis of compound **1**, **2**, **3**, and **4**, respectively. After deprotection of Fmoc group, Fmoc-Orn(alloc)-OH (0.3 mmol, 3 equiv) was coupled with the amino acid on the resin (Scheme S1). After deprotection of Fmoc group, coupling of 4-carboxyphenylboronic acid pinacol ester was performed by the following procedure. 4-carboxyphenylboronic acid pinacol ester (75 mg, 0.3 mmol), HOBt (40 mg, 0.3 mmol) and DIC (47 µL, 0.3 mmol) in DMF (3mL) were added into the resin and the resulting solution containing the resin was stirred for 4 h at room temperature. The deprotection of alloc group of the side chain of ornithine was carried out by the following literature procedure.[45] 1-Pyreneacetic acid (78 mg, 0.3 mmol), HOBt (40 mg, 0.3 mmol) and DIPC (47 µL, 0.3 mmol) in DMF (3mL) were added into the resin and the resulting solution was mixed for 4 h at room temperature. Deprotection and cleavage of the compounds from the resin was achieved by treatment with a mixture of TFA/TIS/H_2O (95:2.5:2.5, v/v) at room temperature for 5 h. After filtration and washing of the resin by TFA, a gentle stream of nitrogen was used to remove the excess TFA. The crude was triturated with diethyl ether chilled at -20 °C and then centrifuged at 3000 rpm for 10 min at -10 °C. The crude product was purified by prep-HPLC with a Vydac C_{18} column using water (0.1% TFA)-acetonitrile (0.1% TFA) gradient to give >79% yield. The successful synthesis was confirmed by ESI mass spectrometry (Platform II, micromass, Manchester,

View Article Online
DOI: 10.1039/C6NJ03830A

UK) and its homogeneity (>98%) was confirmed by reverse phase analytical HPLC with a C18 column:

Compound 1. White solid, Yield : 79 %; t_R = 44 min (H_2O/CH_3CN); mp 260–262 ºC; ^{1}H NMR (400 MHz, DMSO-d_6) δ: 10.8 (s, 1H), 8.43 (d, *J* = 8.4 Hz, 1H), 8.36 (d, *J* = 8.4 Hz, 1H), 8.25 (d, *J* = 8.4 Hz, 1H), 8.23–8.19 (m, 3H), 8.17 (d, *J* = 8.4 Hz, 1H), 8.15–8.12 (m, 2H), 8.17 (d, *J* = 8.4 Hz, 1H), 7.91 (d, *J* = 8.4 Hz, 1H), 7.87–7.85 (m, 2H), 7.82–7.80 (m, 2H), 7.56 (d, *J* = 8.5 Hz, 1H), 7.12 (brs, 1H), 7.05–6.99 (m, 2H), 6.92 (t, *J* = 8.5 Hz, 1H), 4.5–4.4 (m, 2H), 4.2 (s, 2H), 3.19–3.0 (m, 4H), 1.8–1.7 (m, 2H). ^{13}C NMR (50 MHz, DMSO-d_6) δ: 173.9, 172.1, 170.7, 167.4, 138.2, 136.6, 136.0, 134.5, 131.7, 131.4, 131.0, 130.3, 129.6, 129.3, 128.1, 127.8, 127.4, 127.11, 126.8, 125.7, 125.5, 125.4, 124.7, 124.7, 124.6, 124.1, 121.4, 119.1, 118.8, 111.8, 110.6, 54.1, 53.8, 39.5, 39.1, 29.7, 28.3, 26.7, ESI-Mass (m/z) calculated for $C_{41}H_{38}BN_5O_6$ [M + Na^+]$^+$, 730.28; found, 730.16. Elemental analysis (calcd, found for $C_{41}H_{38}BN_5O_6$): C (69.59, 66.07), H (5.41, 5.11), N (9.90, 10.75).

Compound 2. White solid, Yield : 78 %; t_R = 49 min (H_2O/CH_3CN); mp 269–270 ºC; ^{1}H NMR (400 MHz, DMSO-d_6) δ: 8.42 (d, *J* = 8.5 Hz, 1H), 8.35 (d, *J* = 8.4 Hz, 1H), 8.26 (d, *J* = 8.4 Hz, 1H), 8.24–8.19 (m, 3H), 8.15 (d, *J* = 8.4 Hz, 1H), 8.13–8.11 (m, 4H), 8.08–8.0 (m, 1H), 7.99 (d, *J* = 8.5 Hz, 1H), 7.99 (d, *J* = 8.4 Hz, 1H), 7.89–7.8 (m, 5H), 7.66 (d, *J* = 8.4 Hz, 1H), 7.55–7.50 (m, 2H), 7.38 (s, 1H), 7.29 (d, *J* = 8.5 Hz, 1H), 7.28–7.20 (m, 1H), 7.13 (s, 1H), 4.60–1.52 (m, 1H), 4.39–4.30 (m, 1H), 4.16 (s, 2H), 3.60–3.58 (m, 1H), 3.30–3.21 (m, 1H), 3.10–2.90 (m, 1H), 1.70–1.60 (m, 2H), 1.45–1.30 (m, 2H). ^{13}C NMR (50 MHz, DMSO-d_6) δ: 173.5, 172.1, 170.6, 167.4, 135.7, 134.3, 134.2, 133.8, 131.4, 131.3, 130.8, 130.2, 129.4, 129.1, 127.9, 127.7, 127.4, 127.3, 127.0, 126.7, 126.6, 126.0, 125.7, 125.6, 125.4, 125.2, 124.6, 124.4, 124.4, 124.2, 54.1, 53.7, 39.2, 38.9, 35.0, 29.2, 26.3, ESI-Mass (m/z) calculated for $C_{43}H_{39}BN_4O_6$ [M + H^+]$^+$, 719.30; found, 718.38; Elemental analysis (calcd, found for $C_{43}H_{39}BN_4O_6$): C (71.87, 70.66), H (5.47, 5.51), N (7.80, 7.37).

Compound 3. White solid, Yield : 81 %; t_R = 43 min (H_2O/CH_3CN); mp 265–266 ºC; ^{1}H NMR (400 MHz, DMSO-d6) δ: 8.45 (d, *J* = 8.5 Hz, 1H), 8.35 (d, *J* = 8.4 Hz, 1H), 8.25 (d, *J* = 8.5 Hz, 1H), 8.21–8.20 (m, 3H), 8.18 (d, *J* = 8.4 Hz, 1H), 8.15–8.13 (m, 4H), 8.10–8.05 (m, 1H), 8.01 (d, *J* = 8.4 Hz, 1H), 8.95–8.80 (m, 5H), 7.39 (s, 1H), 7.0–7.05 (m, 4H), 4.55–4.39 (m, 2H), 4.18 (s, 2H), 3.10–2.96 (m, 3H), 2.89–2.8 (m, 1H), 1.75–1.62 (m, 2H), 1.5–1.35 (m, 2H). ^{13}C NMR (50 MHz, DMSO-d_6) δ: 172.9, 171.5, 170.1, 166.9, 137.9, 135.4, 134.0, 131.2, 130.9, 130.5, 129.8, 129.3, 129.1, 128.8, 128.1, 127.5, 127.3, 126.9, 126.6, 126.3, 125.2, 125.0, 124.9, 124.2, 124.2, 53.7, 53.6, 39.9, 39.7, 39.5, 29.0, 26.1, ESI-Mass (m/z) calculated for $C_{39}H_{37}BN_4O_6$ [M + H^+]$^+$, 669.28; found, 668.26; Elemental analysis (calcd, found for $C_{39}H_{37}BN_4O_6$): C (70.07, 68.17), H (5.58, 5.53), N (8.38, 7.88).

Compound 4. White solid, Yield : 80 %; t_R = 35 min (H_2O/CH_3CN); mp 247–248 ºC; ^{1}H NMR (400 MHz, DMSO–d_6) δ: 8.94 (s, 1H), 8.52 (d, *J* = 8.5 Hz, 1H), 8.34 (d, *J* = 8.4, Hz, 1H), 8.20 (d, *J* = 8.6 Hz, 1H), 8.19–8.18 (m, 3H), 8.17 (d, *J* = 8.4 Hz, 1H), 8.14–8.10 (m, 4H), 8.05–8.0 (m, 1H), 7.95 (d, *J* = 8.4 Hz, 1H), 7.85–7.79 (m, 5H), 7.32 (d, *J* = 8.6 Hz, 2H), 7.23 (s, 1H), 4.51–4.48 (m, 1H), 4.36–4.31 (m, 1H), 4.14 (s, 2H), 3.09–3.06 (m, 3H), 2.95–2.90 (m, 1H), 1.75–1.69 (m, 2H), 1.58–1.40 (m, 2H). ^{13}C NMR (50 MHz, DMSO-d_6) δ: 171.8, 171.7, 170.0, 167.0, 135.0, 133.8, 130.9, 130.7, 130.2, 129.6, 128.9, 128.5, 127.3, 127.1, 126.7, 126.4, 126.1, 125.0, 124.8, 124.7, 124.0, 123.9, 123.8, 53.7, 51.2, 39.7, 39.5, 39.2, 28.5, 26.0, ESI-Mass (m/z) calculated for $C_{36}H_{35}BN_6O_6$ [M + H^+]$^+$, 659.27; found, 659.23; Elemental analysis (calcd, found for $C_{36}H_{35}BN_6O_6$): C (65.66, 56.26), H (5.36, 4.53), N (12.76, 10.00).

General fluorescence measurements

A stock solution of compounds at the concentration of 1.0 × 10^{-3} M were prepared in DMSO/water (1:1, v/v), and stored in a cold and dark place. The concentration of stock solution was confirmed by UV absorbance at 342 nm for pyrene. Fluorescence emission spectrum of the sample in a 10 mm path length quartz cuvette was measured in 50 mM phosphate buffer solution at pH 7.4 using a PerkineElmer luminescence spectrophotometer (model LS 55). Emission spectra of the compound in the presence of sugars and diol were measured by excitation with 342 nm for pyrene.

Determination of association constant

The association constant for the 1:1 complex was calculated based on the titration curve of the fluorescent chemosensor with sugar. Association constants (K_a) was determined by a nonlinear least squares fitting of the data with the following equation.[35]

$$I = \frac{I_{min} + I_{max}K_a[S]}{1 + K_a[S]} + k'_a[s]$$

Where I_{min} and I_{max} are the initial (no sugar) and final (plateau) fluorescence intensities of the titration curves and k_a' is slope of the linear equation for the fitting of the linearly increased emission intensity as function of the concentration of sugar.

Measurement of the size of the aggregates of the compounds in solutions

The size distribution of the aggregates of compounds in aqueous solution was characterized by using a particle size analyzer (Brookhaven Instruments Corporation, New York, USA, model 9863) equipped with He-Ne laser (633 nm). The measurements of the aggregates in the solution were carried out by 90º dynamic light scattering at 25ºC. Compound (30 μM) was dissolved in 50 mM phosphate buffer solution containing DMSO at pH 7.4 for the size measurement.

Transmission Electron Microscopy (TEM) measurements

Transmission electron microscopy (TEM) was performed using a Philips CM 200 operated at an acceleration voltage of 120 kV. The samples were prepared by dropping 5 μL of **1** (0.5 mM) in aqueous buffered (50 mM phosphate, pH 7.4) solution on a 300-mesh copper grid coated with carbon followed by staining with phosphotungstic acid (2 wt%). The TEM grid was completely dried in the air before TEM measurements were conducted.

Determination of detection limit

View Article Online
DOI: 10.1039/C6NJ03830A

The detection limit was calculated based on the fluorescence titration. To determine the S/N ratio, the emission intensity of dipeptides without D-fructose was measured by ten times and the standard deviation of blank measurements was determined. Three independent duplication measurements of emission intensity were performed in the presence of D-fructose and each average value of the intensities was plotted as a concentration of D-fructose for determining the slope. The detection limit is then calculated with the following equation.[46]

Detection limit = $3\sigma/m$

Where, σ is the standard deviation of the emission intensity of probe and m is the slope between the emission intensity vs. concentration.

Results and Discussion

Design of the self-assembled peptides bearing phenylboronic acid

The assembly and/or disassembly of the self-assembled peptides (**1**–**4**) triggered by sugar were synthesized, as shown in Figure 1. Arylboronic acid as a receptor was conjugated with the peptides because aryl-boronic acid formed reversible covalent adducts with diol compounds including monosaccharides in aqueous solutions and several artificial receptors using arylboronic acid based on various organic compounds, polymers, proteins, and DNA were reported for the recognition of various analytes including saccharides and glycosylated biomolecules.[23–36,47–49] A pyrene fluorophore was incorporated into the dipeptides for the ratiometric detection because the pyrene fluorophore has interesting photophysical properties such as high fluorescence quantum yield and dual fluorescence emission (monomer emission at 376 nm and excimer at 470 nm) depending on the proximity between two pyrene fluorophores.[50,51]

As shown in Figure 1, we synthesized the dipeptides (**1**–**4**) bearing a phenylboronic acid in which the second amino acid was Trp, (3-(Naphthyl)-L-alanine), Phe, and His among aromatic amino acids, to have different self-assembled properties by the change of the hydrophobicity and the structure of the 2nd amino acid. When the peptides bearing a phenylboronic acid might interact with the hydrophilic sugars or hydrophobic diols and form covalent adducts, the peptides might assemble or disassemble depending on the self-assembly property of the covalent adducts and exhibit the change of monomer emissions and excimer emissions depending on the proximity between the pyrene fluorophores.

The peptides (**1**–**4**) with high purity were easily synthesized in solid phase synthesis with high yields.[44] The detailed procedure for the synthesis and characterization of the pyrene labelled peptides were described in the experimental section (Figure S1–S20). The high purity (> 98%) of the peptide was confirmed by analytical HPLC with a C_{18} column and ESI mass spectrometer.

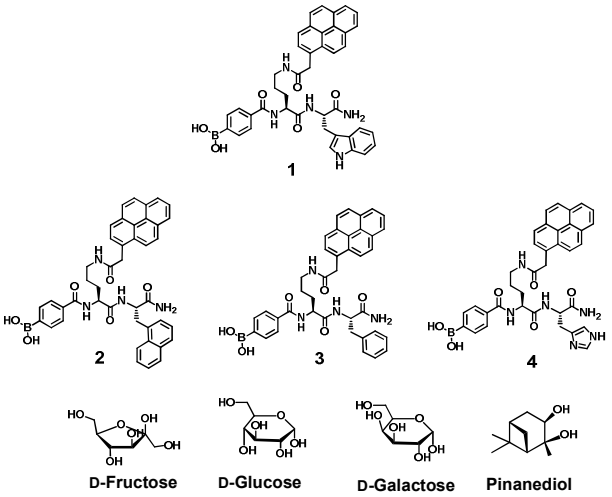

Figure 1. Structures of compound **1**–**4**, monosaccharides, and pinanediol.

Fluorescence emission spectra and the size and shape analysis of the peptides in aqueous buffered solutions containing DMSO

We measured the fluorescence emission spectra of the peptides (**1**–**4**) in aqueous buffered solution (50 mM phosphate pH 7.4) containing different volume percentage of DMSO because amphiphilic peptides dissolved well in DMSO. As shown in Figure 2, **1** displayed a relatively strong excimer emission at 470 nm and weak monomer emissions at 377 and 396 nm in aqueous solution containing 1 % (v/v) DMSO. As the volume percent of DMSO increased from 1 to 10 % (v/v), the excimer emission significantly decreased and the monomer emission considerably increased. The strong pyrene excimer emissions indicated that **1** might aggregate in aqueous solution containing low percentages of DMSO. However, the low excimer emission in aqueous solutions containing high percentages of DMSO suggests that the peptides did not aggregate in this solvent condition.

2 showed significant monomer emissions at 377 and 396 nm and a relatively weak excimer emission in aqueous solution at physiological pH containing 1% DMSO. As the volume percent of DMSO increased from 1 to 20 % in the solution containing **2**, the monomer emission significantly increased and the excimer emission slightly decreased (Figure 2). About 15 % DMSO was enough for the complete disappearance of excimer emissions in aqueous solution. As the volume percent of DMSO increased from 1 to 15%, the monomer emission of **3** significantly increased and the excimer emission decreased (Figure S21). About 3 % DMSO was required for the complete disappearance of excimer emission of **3** in aqueous solution. **4** in which the second amino acid was His, exhibited only monomer emission in 100 % aqueous solution at pH 7.4 and aqueous solution containing high percentages of DMSO (Figure S21). **4** did not aggregate even in 100% aqueous solutions, resulting in only monomer emissions because hydrophilic **4** might not aggregate.

View Article Online
DOI: 10.1039/C6NJ03830A

NJC

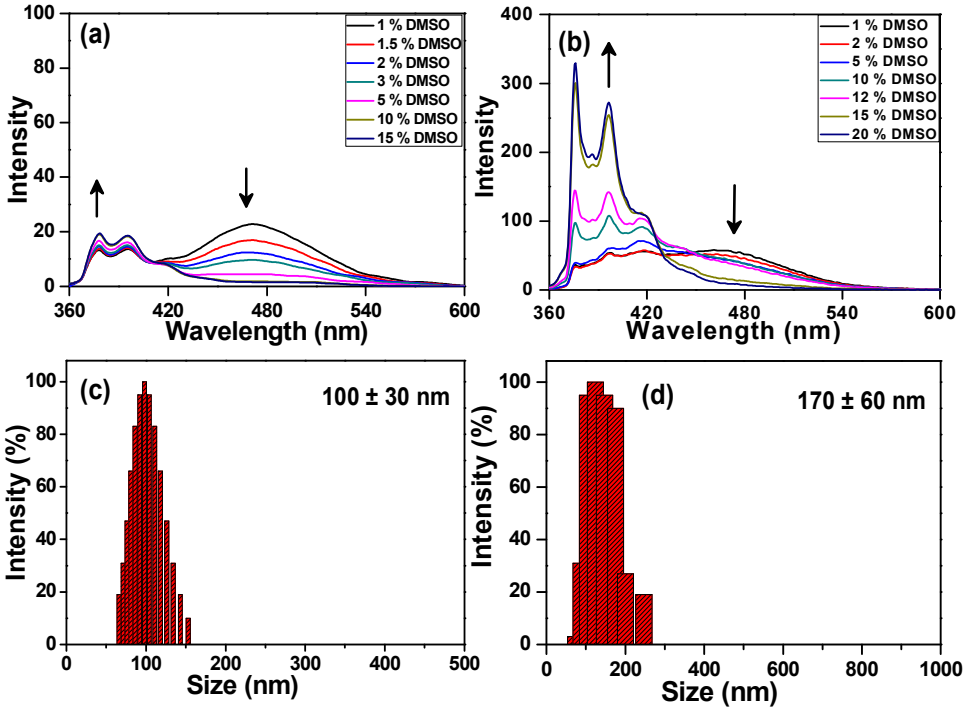

Figure 2. Fluorescence spectra of (a) **1** (10 μM) and (b) **2** (10 μM) in aqueous buffered solution (50 mM phosphate, pH 7.4) containing different percentage of DMSO (λ_{ex} = 342 nm, slit = 12/2.5 nm). Size distribution of DLS measurements of (c) **1** (30 μM) and (d) **2** (30 μM) in aqueous buffered solution containing 3 % and 10 % DMSO, respectively.

We investigated the size of the self-aggregates of the peptides in aqueous buffered solution containing DMSO using a dynamic light scattering (DLS) measurement. As shown in Figure 2, **1** and **2** that showed a significant excimer emission in solutions formed aggregates with an average diameter of ca. 100 nm and 170 nm, respectively. Similarly, **3** that exhibited excimer emissions in solutions also formed nano-aggregates with an average diameter of ca 90 nm in aqueous buffered solution (Figure S22). DLS result indicates that **4** which did not show excimer emissions in 100% aqueous solutions did not form aggregates in this solvent condition (Figure S22).

The overall result suggests that the hydrophobicity of the second amino acid in the peptides play a critical role for the self-aggregations and excimer emissions in aqueous solution. The retention time on C_{18} column might correlate well with the hydrophobicity.[52] According to the retention time of the peptides, the order of hydrophobicity was **2** > **1** > **3** > **4**. More hydrophobic peptides required more DMSO in aqueous solutions for the observation of a little excimer emission. The maximum excimer intensity of the peptides may correlate with the hydrophobicity of the peptides; the maximum excimer emission intensity at 470 nm was 23 for **1**, 50 for **2**, and 20 for **3**, respectively.

UV-visible spectra of **1** in aqueous solutions containing different percentage of DMSO showed that as the volume percentage of DMSO in aqueous solutions increased, a considerable increase of absorbance at 343 nm was observed (Figure S23). As the peptide self-aggregated in solutions, the pyrene fluorophore might be overlapped and the absorbance corresponding to the pyrene might decrease. As the percentage of DMSO increased, the self-aggregates did not form, resulting in the increase of the absorbance of the pyrene. UV-visible spectra of **2** and **3** indicated that the absorbance at 343 nm increased as the volume percentage of DMSO increased. This indicates that **1**–**3** did not aggregate as the percentage of DMSO in aqueous solution increased. UV-visible spectra of **4** revealed that the absorbance at 343 nm was not considerably changed as the volume percentage of DMSO in the solution increased (Figure S23). This indicated that as relatively hydrophilic peptide (**4**) did not aggregate in aqueous solutions containing different volumes of DMSO, the absorbance of the pyrene at 343 nm did not change considerably.

Furthermore, we investigated the structures of the self-assembled aggregates of **1** by transmission electron microscopy (TEM). As shown in Figure 3, **1** self-aggregated and formed vesicle-like structures in aqueous buffered solution. The size of vesicle ranged from 50 nm to 80 nm, which was smaller than that measured by DLS maybe due to the dehydration process. Interestingly, when the concentration of **1** was increased to 2 mM, the formation of nanofibrils with the length of 100~200 nm was observed (Figure 3b). This suggests that if the concentration of the peptide reaches to certain high

View Article Online
DOI: 10.1039/C6NJ03830A

concentration, the formation of nanofibrils might be predominant. This result was consistent with the fact that the self-assembled dipeptide (PhePhe) formed different nanostructures such as nanoparticles, nanofibril, nanotubular aggregates in different solvent conditions.[2,39]

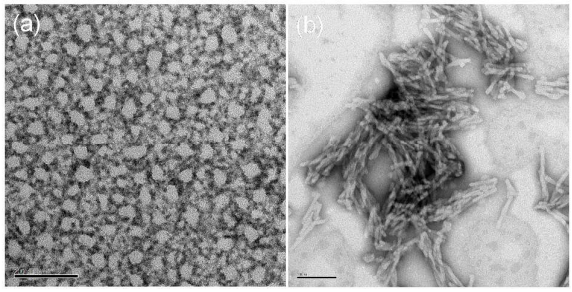

Figure 3. TEM images of **1** (a) (0.5 mM) and (b) (2 mM) in aqueous buffered solution (50 mM phosphate buffer, pH 7.4). The samples were negatively stained with 2% phosphotungstic acid. The bar represents 200 nm (a) and 100 nm (b).

Fluorescence emission spectra of 1–4 in the presence of monosaccharide

The fluorescence emission responses of **1**-**3** to monosaccharides were investigated in aqueous buffered solution at pH 7.4 (Figure 4). **1** displayed a strong excimer emission band at 470 nm and weak monomer emissions at 377 and 396 nm in aqueous buffered solution (50 mM phosphate, pH 7.4) containing 1% (v/v) DMSO. Upon addition of D-fructose, a significant decrease of pyrene excimer emission at 470 nm and a concomitant increase of pyrene monomer emissions at 377 and 396 nm were observed. The intensity ratio (I_{377}/I_{470}) was significantly changed from 0.60 to 15 as the concentration of D-fructose increased from 0 to 7.5 mM. Approximately 7.5 mM of D-fructose was necessary for the complete disappearance of the pyrene excimer. Similarly, **2** also showed a strong excimer emission at 470 nm and weak monomer emissions at 376 and 396 nm in aqueous buffered solution (50 mM phosphate, pH 7.4) containing 5% (v/v) DMSO. Upon addition of D-fructose, a significant increase of the monomer emissions at 377 nm and 396 nm and considerable decrease of the excimer emission band at 470 nm were observed with a clear isoemission point at 432 nm. The intensity ratio (I_{377}/I_{470}) increased from 0.71 to 16 as the concentration of D-fructose increased and about 20 mM of D-fructose was required for the complete disappearance of the excimer emissions.

The fluorescence emission spectra of **3** in aqueous buffered solution (50 mM phosphate, pH 7.4) containing 0.5% (v/v) DMSO, displayed weak excimer emission at 470 nm. Upon addition of D-fructose to the solution of **3**, a significant increase of monomer intensity at 376 nm and 396 nm and slightly decrease of excimer emission intensity were observed (Figure 4). The intensity ratio (I_{376}/I_{470}) between the monomer and excimer emission increased from 2.2 to 26 and 20 mM of D-fructose was enough for the complete change of the intensity ratio. The results suggest that the covalent bonding with D-fructose might induce disassembly of supramolecular nanostructures of the peptides (**1**–**3)** in aqueous solutions.

We also investigated the fluorescence responses of **1**, **2**, and **3** to D-glucose and D-galactose, respectively (Figure S24–S26). Although they required a high concentration of D-glucose and D-galactose for the fluorescent emission changes, the addition of D-glucose and D-galactose at physiological pH resulted in the increase of monomer emission intensity and decrease of the excimer emission, respectively. This suggests that the disassembly of the self-assembled peptide aggregates (**1**–**3**) was triggered by monosaccharides in aqueous solution. As **4** was dissolved well in distilled water, the fluorescence spectrum was measured in 100 % aqueous solution (50 mM phosphate, pH 7.4) without organic solvent. As shown in Figure 4, **4** displayed strong emission intensities at 376 and 396 nm, corresponding to the typical monomer emission bands of the pyrene, which indicated that **4** might not aggregate in 100% aqueous solutions. Upon addition of D-fructose, the monomer emission at 376 and 396 nm was gradually increased. About 6 mM D-fructose was required to completely change the emission intensity in aqueous solution. Similar monomer emission enhancement of **4** was observed in the presence of D-glucose and D-galactose, respectively (Figure S27).

View Article Online
DOI: 10.1039/C6NJ03830A

NJC

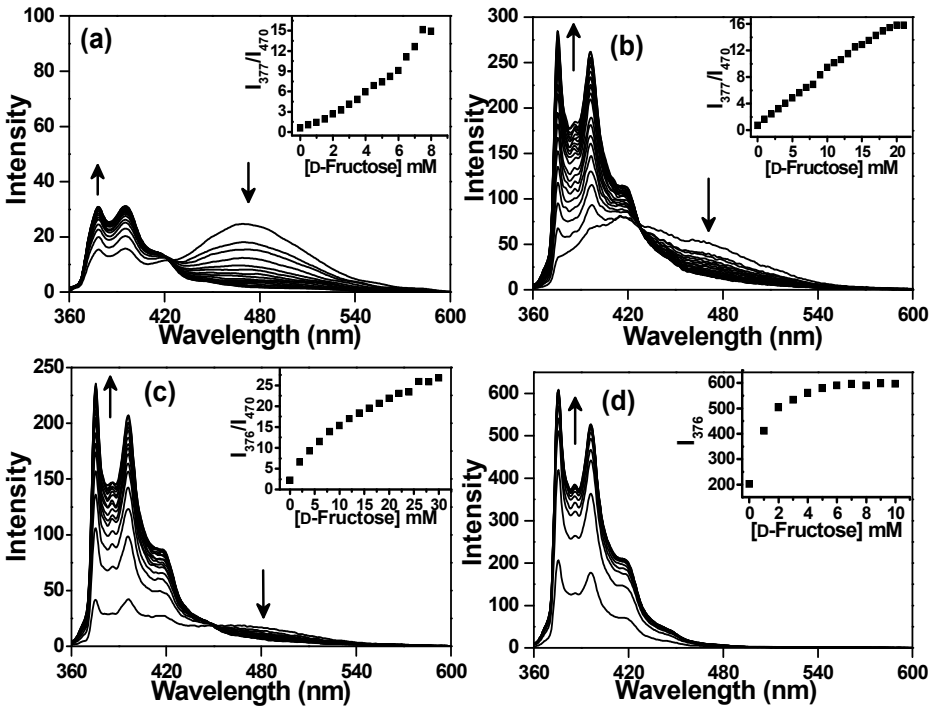

Figure 4. Fluorescence spectra of (a) **1** (b) **2** (c) **3**, and (d) **4** upon the gradual addition of D-fructose in aqueous buffered solution (50 mM phosphate, pH 7.4) containing DMSO solvent (1 %, 5 %, 0.5 % and 0 %, respectively). The concentration of peptides is 10 μM.

UV−visible titration experiment was carried out (Figure S28). In the UV−visible absorption titration of **1** with D-fructose, a considerable increase in absorbance at 343 nm corresponding to the pyrene fluorophore was observed as the concentrations of D-fructose increased. Similarly, **2** and **3** also showed a considerable increase of the absorbance at 343 nm in the presence of D-fructose (Figure S28). The results indicated that after the peptides (**1**–**3**) were complexed with D-fructose, the aggregates might disassemble, resulting in the increase of the absorbance of pyrene. However, the absorbance spectra of **4** were not changed in the presence of D-fructose. As **4** did not form self-aggregates in aqueous solution even in the absence of sugar, disassembly could not be triggered by covalent bonding with D-fructose.

We also investigated whether the nanoparticles of the self-assembled peptide disassembled in the presence of hydrophilic sugars or not. Interestingly, DLS measurements of the peptide in the presence of D-fructose revealed that the addition of D-fructose induced the disassembling of the nanoparticles of **1**–**3**. (Figure S29). Furthermore, upon addition of D-fructose, the vesicle-like nanostructures disappeared in TEM, which suggests that the supramolecular nanostructures of **1** were disassembled by covalent bonding with hydrophilic D-fructose.

Fluorescence emission spectra and the size distributions of the peptides of 1–4 in the presence of a hydrophobic diol

When the peptides formed a covalent bonding with hydrophilic sugars, the nanoparticles of the peptide disassembled, resulting in the decrease of the excimer emission and increase of monomer emissions. Thus, we investigated whether the binding of a hydrophobic diol compound would affect the fluorescence emission spectrum and the formation of the nanoparticles.

As shown in Figure 5, the addition of pinanediol to the solution containing **1** induced a significant increase of the excimer emission at 470 nm and a slight decrease of the monomer emissions at 376 nm. The intensity ratio I_{470}/I_{376} increased from 1.8 to 31 and just 80 μM of pinanediol was enough for the complete change of both monomer and excimer emission intensities. Upon addition of increasing concentration of pinanediol to the solution of **2**, the increase of excimer emission and the decrease of monomer emissions were observed (Figure S30). About 60 μM of pinanediol was required for the saturation of the intensity ratio change. Upon addition of pinanediol into the solution of **3**, a significant increase in the pyrene excimer emission at 470 nm and significant decrease in the pyrene monomer emissions were observed (Figure 5). The intensity ratio (I_{470}/I_{376}) between the excimer and monomer emissions changed from 0.2 to 7. The results indicate that the covalent bonding of pinanediol with **1**–**3** may stabilize the nanoparticles in aqueous solutions, resulting in the enhanced excimer emission and a concomitant decrease of the monomer emission.

View Article Online
DOI: 10.1039/C6NJ03830A

NJC

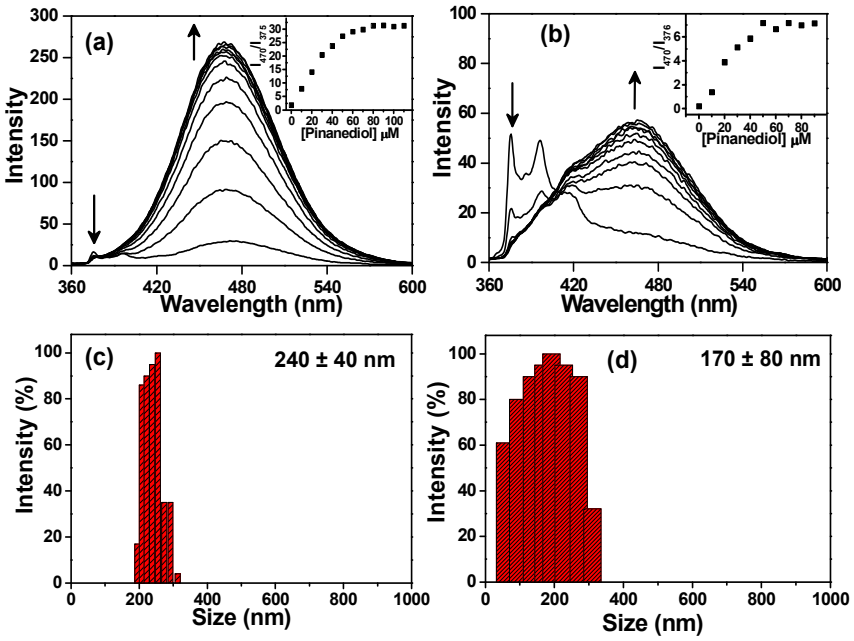

Figure 5. Fluorescence spectra of (a) **1** (10 μM) and (b) **3** (10 μM) upon the gradual addition of pinanediol in aqueous buffered solution (50 mM phosphate, pH 7.4) containing 1% and 0.5 % DMSO, respectively (λ_{ex} = 342 nm, slit = 12/2.5 nm). Particle size distribution of (c) **1** (30 μM) and (d) **3** (30 μM) in aqueous buffered solution containing 3% DMSO.

UV−vis titration of **1**–**3** with pinanediol was carried out (Figure S31). Upon addition of pinanediol to the solution of **1**–**3**, a significant decrease in the absorbance at 343 nm corresponding to the pyrene and red shift were observed, which indicated the overlap of the pyrene fluorophores was induced by the covalent bonding of pinanediol with **1**–**3**.[50,51]

Even though **4** did not show excimer emission in aqueous solution, the addition of pinanediol induced the significant increase of the excimer emission and the decrease of monomer emissions (Figure S32). The relatively hydrophilic peptide (**4**) required about 200 μM of pinanediol for the complete change of the excimer emission and monomer emissions. During the UV-visible titration of **4** with pinanediol, a significant decrease of the absorbance at 343 nm and a red shift of the absorption spectra were observed (Figure S32). This suggests that after complexation of **4** with pinanediol, the pyrene fluorophores overlapped, resulting in the decrease of the absorbance at 343 nm and an increase in excimer emission.

We investigated whether the addition of pinanediol induced the change of the nanoparticles of **1**–**4** or not. DLS experiments indicated that the size of the nanoparticles increased in the presence of pinanediol. The self-assembled peptides (**1**, **2**, and **3**) formed nanoparticles with the average size of 100 nm, 170 nm, and 90 nm in the absence of diol compounds, respectively. Upon addition of pinanediol to the solution of **1**, the average size of the nanoparticles increased from 100 nm to 240 nm (Figure 5). Similarly, the size of nanoparticles of **2** and **3** increased in the presence of pinanediol. The increase of the average size of the nanoparticles was consistent well with the increase of the excimer emissions (Figure S33). When the self-assembled peptides formed covalent adducts with the hydrophobic diol, the size of the resulting nanoparticles increased and the overlapped pyrene fluorophore increased, resulting in the increase of the excimer emissions.

The effect of hydrophobic pinanediol on the assembly of **4** was much significant. **4** did not form nanoparticles even in 100% aqueous solution without organic cosolvent. However, upon addition of pinanediol, the nanoparticles with the average size of 130 nm were observed with the significant excimer emission (Figure S33). The result suggested that the assembly of the peptide for the nanoparticles could be triggered by the addition of the hydrophobic diol compound.

Furthermore, we investigated the nanostructure of the self-assembled peptide (**1**) in the presence of pinanediol by using a transmission electron microscopy (TEM). Upon addition of hydrophobic pinanediol, the vesicle-like structures in the absence of pinanediol were converted to the fibrils (Figure 6). The average size of the fibrils was much larger than those measured by DLS. This is because small fibrils induced by covalent bonding with the hydrophobic pinanediol might convert to larger fibrils during the dehydration process or larger fibrils could not be well detected by DLS measurements due to the precipitations.

We also investigated whether **4** formed nanoparticles in the presence of pinanediol or not. Upon addition pinanediol into the solution, the nanoparticle structures were clearly observed in

View Article Online
DOI: 10.1039/C6NJ03830A
NJC Paper

TEM images (Figure 6b). This suggests that the covalent bonding of the hydrophilic peptide (**4**) with a hydrophobic diol induce the self-aggregation and formation of nanoparticles.

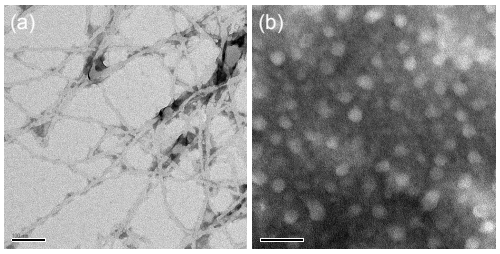

Figure 6. TEM images of (a) **1** (0.5 mM) and (b) **4** (0.5 mM) in the presence of pinanediol in aqueous buffered solutions (50 mM phosphate, pH 7.4) containing CH_3CN. Samples were negatively stained with 2% phosphotungstic acid. The bar represents 100 nm (a) and 50 nm (b).

Binding affinity, detection limit, and selectivity for the diol compounds

The binding stoichiometry was investigated by ESI mass spectrometry. After adding D-fructose to the solution of **1**, a new peak at 850.31 (m/z) appeared. This peak corresponded to [**1**·D-fructose - $2H_2O$ - H^+]$^-$ (Figure S34), which confirmed that **1** formed a 1:1 complex with D-fructose. ESI mass spectrum for the sample containing **2** and D-fructose showed that the peak at 862.42 (m/z) corresponding to [**2**·D-fructose - $2H_2O$ - H^+]$^-$ was observed (Figure S35). This result supports that **2** also formed a 1:1 complex with D-fructose. In general, one phenylboronic acid of the receptor formed a 1:1 complex with various diol compounds.[28–36]

Assuming the formation of a 1:1 complex, the association constant (K_a) of **1**–**4** for sugar and pinanediol were calculated based on the titration curve by nonlinear least square fitting (Figure S36).[35] The fitting of titration curves provided less than 5% errors, which also confirmed the 1:1 binding stoichiometry of the peptide. Table 1 summarized K_a values and detection limits of **1**–**4** for monosaccharides and pinanediol. The K_a values revealed that all peptides showed a high selectivity for fructose among sugars. The order of K_a values (D-fructose>D-galactose>D-glucose) of **1**–**4** for the sugar is similar to the order of the association constants of phenylboronic acid for the sugars.[53] The order of K_a values of **1**–**4** for the sugars correlated with the order of K_a values of the reported fluorescent probes using phenylboronic acid[23,24,27], which indicates that the boronic ester formation between the phenylboronic acid moiety of the peptides and the diol compounds induced the change of the fluorescent spectra and nanostructures. The binding affinity of the boronic acid for sugar was determined by the orientation and relative position of hydroxyl groups of the sugar. In general, the binding affinity for D-fructose was most potent because D-fructose existed as a furanose form with a relative high percentage in aqueous solutions that contained a syn-periplanar pair of hydroxyl groups.[27] The association constants of **1**–**4** for pinanediol were calculated based on the titration curve (Figure S37). The binding affinity of the peptides for pinanediol is much higher than those for the monosaccharides. The high K_a values for pinanediol may be due to the position and configuration of the diol of pinanediol that formed a stable boronic ester form.[23,24,47]

Considering the applications for the detection of fructose, we measured the detection limits and the linear response ranges of the changes in intensity ratio by fructose. As shown in Fig. S38, **1**-**3** showed sensitive linear ratiometric responses to sub-molar concentrations (100~800 μM) of D-fructose in aqueous buffered solution. The detection limit was calculated based on the linear relationships between the intensity ratio (I_{378}/I_{475}) and the concentration of D-fructose. Even though **3** did not have the highest association constant for fructose among the peptides (**1**-**3**) that showed a ratiometric response to sugar, the sensitivity of **3** was the greatest among the peptides so **3** had the lowest detection limit for D-fructose. **3** had some advantages for the detection of D-fructose because **3** aggregated in aqueous solutions without organic cosolvent and showed the most sensitive ratiometric response to D-fructose.

As shown in Figure 7, **3** showed a highly selective ratiometric response to D-fructose among monosaccharide, As the concentration of fructose increased, the intensity ratio (I_{376}/I_{470}) significantly increased from 2.2 to 26 and the intensity at 376 nm increased from 40 to 240. The large enhancement of the emission by fructose and sensitive ratiometric response to fructose provided a selective detection of fructose among monosaccharides in aqueous solutions.

Table 1. Apparent association constants (K_a) and detection limits of **1**–**4** for diol compounds.

Peptides	K_a [M^{-1}]				Detection limit for D-fructose [M]	Detection limit for pinanediol [M]
	D-Fructose	D-Galactose	D-Glucose	Pinanediol		
1	1.15×10^3	1.01×10^2	41	61.4×10^3	9.74×10^{-5}	2.13×10^{-7}
2	0.14×10^3	0.24×10^2	14	34.7×10^3	9.55×10^{-5}	9.96×10^{-7}
3	0.22×10^3	0.45×10^2	21	73.2×10^3	8.66×10^{-5}	3.14×10^{-7}

View Article Online
DOI: 10.1039/C6NJ03830A
Paper NJC

4	1.32×10^3	1.40×10^2	46	21.3×10^3	2.31×10^{-5}	4.20×10^{-6}

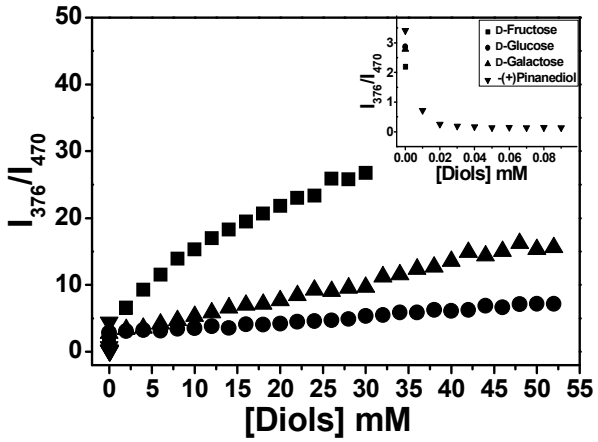

Figure. 7. Emission intensity ratio of **3** (10 μM) upon the addition of D-fructose (■), D-galactose (▲), D-glucose (●), and –(+)–pinanediol (▼) in 50 mM phosphate buffer solution containing 0.5% DMSO at pH 7.4.

Figure 8 presents a visible emission color images of **3** in the presence of sugars and pinanediol under UV light (λ_{em} = 365 nm) with a UV lamp. **3** displayed a blue color in the absence of sugars and pinanediol whereas **3** displayed a violet color in the presence of D-fructose and a brighter cyan color in the presence of pinanediol. This result indicates that the ratiometric probe (**3**) made it possible for the selective detection of fructose among monosaccharides by the naked eye with a UV lamp.

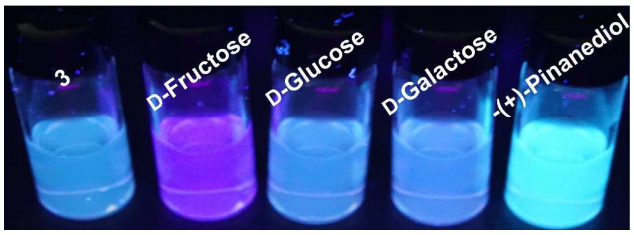

Figure 8. Visible emission color change of **3** (10 μM) in the presence of monosaccharides (20 mM) and pinanediol (0.1 mM) under UV light (λ_{em} = 365 nm).

We proposed how the assembly and disassembly of the self-assembled peptides were controlled by diols compounds. As shown in Scheme 1, **1**–**3** self-aggregated and formed nanoparticles in aqueous solution at physiological pH in which the pyrene fluorophores were close each other, resulting in the excimer emissions. When the hydrophilic sugars such as D-fructose, D-glucose, and D-galactose covalently bonded with the phenylboronic acid of **1**–**3**, the hydrophilicity of the complex increased and the self-aggregates disassembled, resulting in the increase of monomer emissions and a concomitant decrease of excimer emissions. When the hydrophobic pinanediol covalently bonded with the self-assembled peptides **1**–**3**, the hydrophobicity of the complex increased, resulting in the stabilization of nanoparticle structures with the enhancement of excimer emissions which might slowly induce the fibril formation.

As shown in Scheme 1, the peptide (**4**) did not self-aggregate in aqueous solution. When the hydrophobic pinanediol covalently bonded with the peptide (**4**), the resulting covalent adduct with pinanediol self-aggregated and formed nanoparticles, resulting in the increase of excimer emission and decrease of monomer emissions. As the hydrophilic sugar covalently bonded with the peptide (**4**), the monomer emission was significantly increased without the formation of nanoparticles. This enhancement can be explained by the strong quenching effect of phenylboronic acid to the adjacent pyrene fluorophore because phenylboronic acid acted as a quencher for pyrene fluorophore and the tetrahedral boronate form showed a much weaker quenching effect rather than the corresponding boronic acid form.[32]

Herein, we report the discovery of a selective and highly sensitive fluorescent probes based on the self-assembled peptides for fructose in aqueous solutions. In last two decades, the worldwide consumption of fructose and high-fructose corn syrup has increased significantly and the high administration of fructose highly related to the increase of the obesity, diabetes, hypertension, and kidney disease.[54] Thus, the simple and easy detection of fructose in food is important to control of the administration of fructose. Even though several ratiometric fluorescent probes for fructose have been reported, most of them suffered from one of the limitations such as the difficulty of the synthesis, poor solubility in water, low sensitivity (enhancement), and low emission intensity change by fructose.[23-26] The fluorescent probes developed in this work are easy to synthesize and selectively and sensitively detected fructose in aqueous solutions by significant emission intensity changes. Thus, the probes will provide an efficient method for the detection of fructose in aqueous solutions.

Conclusion

We synthesized self-assembled peptides in aqueous solution at physiological pH and demonstrated the disassembly and assembly of supramolecular nanoparticles of the self-assembled peptides controlled by the diol compounds for the ratiometric detection. The amphiphilic peptides (**1**–**3**) self-aggregated and formed vesicle-like nanostructures, resulting in the considerable excimer emission. The covalent bonding of the phenylboronic acid of the peptides (**1**–**3**) with hydrophilic sugars induced disassembly of the nanoparticles, resulted in a decrease of excimer emissions and a concomitant increase of monomer emissions. The covalent bonding of hydrophobic pinanediol with **1**–**3** stabilized the formation of the nanoparticles, resulting in the significant enhancement of excimer emissions and a decrease of monomer emissions. The dipeptide (**4**) did not self-aggregate in aqueous solution and only showed monomer emissions. The assembly of **4** to the nanoparticles which

View Article Online
DOI: 10.1039/C6NJ03830A

exhibited a considerable excimer emission could be triggered by pinanediol. **1**-**3** showed selective ratiometric responses to fructose among sugars and **3** showed the lowest detection limit for fructose. **4** exhibited a selective ratiometric response to pinanediol by the enhancement of excimer emissions at 475 nm and exhibited turn on responses to sugars by the enhancement of monomer emissions at 376 nm. This study revealed that the self-assembled peptides triggered by sugars will be a valuable tool for the sensitive ratiometric detection for sugar in aqueous solutions.

Acknowledgements

This work was supported by Inha University Research Grant.

Notes and references

1 I. W. Hamley, *Soft Matter,* 2011, **7**, 4122–4138.
2 E. Gazit, *Chem. Soc. Rev*., 2007, **36**, 1263–1269.
3 S. Fleming and R. V. Ulijn, *Chem. Soc. Rev.,* 2014, **43**, 8150–8177.
4 H. Hosseinkhani, P. Hong and D. Yu, *Chem. Rev.,* 2013, **113**, 4837−4861.
5 Y.-b. Lim, K.-S. Moon and M. Lee, *Chem. Soc. Rev*., 2009, **38**, 925–934.
6 H. Wang, Z. Yang and D. J. Adams, *Mater. Today*, 2012, **15**, 500–507.
7 A. Lakshmanan, S. Zhang and C. A. Hauser, *Trends Biotechnol.,* 2012, **30**, 155–165.
8 D. Mandal, A. N. Shirazi and K. Parang, *Org. Biomol. Chem*., 2014, **12**, 3544–3561.
9 H. Cui, M. J. Webber and S. I. Stupp, *Biopolymers*, 2010, **94**, 1–18.
10 X. Zhao, F. Pan, H. Xu, M. Yaseen, H. Shan, C. A. Hauser, S. Zhang and J. R. Lu, *Chem. Soc. Rev*., 2010, **39**, 3480–3498.
11 P.-P. Yang, X.-X. Zhao, A.-P. Xu, L. Wang and Hao Wang, *J. Mater. Chem. B*, 2016, **4**, 2662–2668.
12 R. Zou, Q. Wang, J. Wu, J. Wu, C. Schmuck and H. Tian, *Chem. Soc. Rev.,* 2015, **44**, 5200–5219.
13 W. She, K. Luo, C. Zhang, G. Wang, Y. Geng, L. Li, B. He, Z. Gu, *Biomaterials*, 2013, **34**, 1613–1623.
14 M. R. Dreher, A. J. Simnick, K. Fischer, R. J. Smith, A. Patel, M. Schmidt and A. Chilkoti, *J. Am. Chem. Soc*., 2008, **130**, 687–694.
15 M. J. Webber, C. J. Newcomb, R. I. Bitton and S. I. Stupp, *Soft Matter*, 2011, **7**, 9665–9672.
16 A. N. Rissanou, E. Georgilis, E. Kasotakis, A. Mitraki and V. Harmandaris, *Phys. Chem. B*, 2013, **117**, 3962−3975.
17 M. Ikeda, T. Tanida, T. Yoshii, K. Kurotani, S. Onogi, K. Urayama and I. Hamachi, *Nat. Chem*., 2014, **6**, 511–518.
18 A. Ghosh, M. Haverick, K. Stump, X. Yang, M. F. Tweedle and J. E. Goldberger, *J. Am. Chem. Soc*., 2012, **134**, 3647–3650.
19 C. J. Bowerman and B. L. A. Nilsson, *J. Am. Chem. Soc.,* 2010, **132**, 9526–952.
20 H. Xu, A. K. Das, M. Horie, M. S. Shaik, A. M. Smith, Y. Luo, X. Lu, R. Collins, S. Y. Liem, A. Song, P. L. A. Popelier, M. L. Turner, P. Xiao, I. A. Kinloch and R. V. Ulijn, *Nanoscale*, 2010, **2**, 960–966.
21 H. J. Allen and E. C. Kisailus, Glycoconjugates: Composition, Structure and Function, CRC Press, 1992.
22 C. R. Bertozzi and L. L. Kiessling, *Science*, 2001, **291**, 2357–2364.
23 S. D. Bull, M. G. Davidson, J. M. H. Vanden Elsen, J. S. Fossey, A. T. Jenkins, Y. B. Jiang, Y. Kubo, F. Marken, K. Sakurai, J. Zhao and T. D. James, *Acc. Chem. Res*., 2013, **46**, 312–326.
24 R. Nishiyabu, Y. Kubo, T. D. James and J. S. Fossey, *Chem. Commun*., 2011, **47**, 1106–1123.
25 Z. Guo, I. Shin and J. Yoon, *Chem. Commun*., 2012, 5956–5967.
26 H. Fang, G. Kaur and B. Wang, *J. Fluoresc*., 2004, **14**, 481–489.
27 X. Wu, Z. Li, X.-X. Chen, J. S. Fossey, T. D. James and Y.-B. Jiang, *Chem. Soc. Rev*., 2013, **42**, 8032–8048.
28 X. Sun, B. Zhu, D.-K. Ji, Q. Chen, X.-P. He, G.-R. Chen, T. D. James, *ACS Appl. Mater. Interfaces*, 2014, **6**, 10078–10082.
29 Y. Liu, J. Zhu, Y. Xu, Y. Qin and D. Jiang, *ACS Appl. Mater. Interfaces,* 2015, **7**, 11141–11145.
30 M. Elstner, K. Weisshart, K. Mullen and A. Schiller, *J. Am. Chem. Soc.,* 2012, **134**, 8098–8100.
31 T. L. Halo, J. Appelbaum, E. M. Hobert, D. M. Balkin and A. Schepartz, *J. Am. Chem. Soc*., 2009, **131**, 438–439.
32 L. N. Neupane, C. R. Lohani, J. Kim and K.-H. Lee, *Tetrahedron*, 2013, **69**, 11057–11063.
33 Y.-J. Huang, W.-J. Ouyang, X. Wu and Z. Li, *J. Am. Chem. Soc*., 2013, **135**, 1700–1703.
34 Y. Liu, C. Deng, L. Tang, A. Qin, R. Hu, J. Z. Sun and B. Z. Tang, *J. Am. Chem. Soc*., 2011, **133**, 660–663.
35 N. D. Cesare and J. R. Lakowicz, *J. Photochem. Photobiol. A,* 2001, **143**, 39–47.
36 H. S. Mader and O. S. Wolfbeis, *Microchim. Acta*., 2008, **162**, 1–34.
37 B. Valeur, Molecular Fluorescence: Principles and Applications, Wiley-VCH, Weinheim, 2002.
38 J. R. Lakowicz, Topics in Fluorescence Spectroscopy: Probe Design and Chemical Sensing, vol. 4, Plenum Press, New York, 1994.
39 M. Reches and E. Gazit, *Nat. Nanotechnol*., 2006, **1**, 195–200.
40 M. Mandal, S. K. Mandal, M. Ghosh and P. K. Das, *Chem. Eur. J*., 2015, **21**, 12042–12052.
41 T. Hoeg-Jensen, S. Havelund, P. K. Nielsen and J. Markussen, *J. Am. Chem. Soc.,* 2005, **127**, 6158–6159.
42 B. H. Jones, A. M. Martinez, J. S. Wheeler, B. B. McKenzie, L. L. Miller, D. R. Wheeler and E. D. Spoerke, *Chem. Commun*., 2015, **51**, 14532–14535.
43 L. N. Neupane, S. Y. Han and K.-H. Lee, *Chem. Commun*., 2014, **50**, 5854–5857.
44 G. B. Fields and R. L. Nobel, *Int. J. Pept. Protein Res.,* 1990, **35**, 161–214.
45 N. Thieriet, J. Alsina, E. Giralt, F. Guibe and F. Albericio, Tetrahedron Lett., 1997, 38, 7275–7278.
46 G. L. Long and J. D. Winefordner, *Anal. Chem*. 1983. **55**, 713-724.
47 D. G. Hall, Structure, Properties, and Preparation of Boronic Acid Derivatives. Overview of Their Reactions and Applications. Wiley, Weinheim, 2005.
48 W. L. A. Brooks and B. S. Sumerlin, *Chem. Rev*., 2016, **116**, 1375–1397.
49 N. Y. Edwards, T. W. Sager, J. T. McDevitt, E. V. Anslyn, *J. Am. Chem. Soc.*, 2007, **129**, 13575–13583.
50 F. M. Winnik, *Chem. Rev*., 1993, **93**, 587–614.
51 C. Yao, H.-B. Kraatz and R. P. Steer, *Photochem. Photobiol. Sci*., 2005, **4**, 191–199.
52 R. A. Houghten and S. T. Degraw, *J. Chromatogr. A,* 1987, **386**, 223–228.
53 J. Yan, G. Springsteen, S. Deeter and B. Wang, *Tetrahedron,* 2004, **60**, 11205–11209.
54 R. J. Johnson, M. S. Segal and Y. Sautin, *Am. J. Clin. Nutr.,* 2007, **86**, 899–906.